Optimization of $R_{e^+e^-}$ and "freezing" of the QCD couplant at low energies

A. C. Mattingly and P. M. Stevenson

T. W. Bonner Laboratory, Physics Department, Rice University, Houston, Texas 77251

(Received 9 July 1993)

The new result for the third-order QCD corrections to $R_{e^+e^-}$, unlike the old, incorrect result, is nicely compatible with the principle-of-minimal-sensitivity optimization method. Moreover, it leads to infrared fixed-point behavior: the optimized couplant α_s/π for $R_{e^+e^-}$ does not diverge at low energies, but "freezes" to a value 0.26 below about 300 MeV. This provides some direct theoretical evidence, purely from perturbation theory, for the "freezing" of the couplant—an idea that has long been a popular and successful phenomenological hypothesis. We use the "smearing" method of Poggio, Quinn, and Weinberg to compare the resulting theoretical prediction for $R_{e^+e^-}$ with experimental data down to the lowest energies, and find excellent agreement.

PACS number(s): 12.38.Bx, 12.38.Aw, 12.38.Qk, 13.65.+i

I. INTRODUCTION

The calculation [1, 2] of the third-order (next-to-next-to-leading order) QCD corrections to $R_{e^+e^-}$,

$$R_{e^+e^-} \equiv \sigma_{\rm tot}(e^+e^- \to {\rm hadrons})/\sigma(e^+e^- \to \mu^+\mu^-),$$

(1.1)

provides valuable empirical information on the behavior of perturbation theory in QCD. This paper is concerned with "optimized perturbation theory" (OPT) [3], and is motivated by three questions which the $R_{e^+e^-}$ calculation can answer [4].

(1) *Does perturbation theory seem to be well behaved?* Is the third-order "optimized" result in reasonable agreement with the second-order "optimized" result? What can we learn about the error estimate?

(2) *Is the optimized couplant $a \equiv \alpha_s/\pi$ smaller in third order than in second?* The "induced-convergence" picture [5] suggests that the optimized couplant $\bar{a}^{(n)}$, as determined by the nth-order optimization equations, will tend to decrease as the order n increases. In this way "optimization" could lead to a convergent sequence of perturbative approximations, even if the perturbation series in any *fixed* renormalization scheme is divergent [5].

(3) *Does one find infrared fixed-point behavior?* A third-order calculation is a prerequisite for addressing this question in "optimized" perturbation theory, and the answer basically depends upon whether or not the invariant ρ_2 (defined below) is negative [6].

It is striking that, with the originally published third-order result [1], the answer to all three questions was "no", while, with the new, corrected, result [2] the answer to all three questions is "yes." The purpose of this paper is to elaborate on these three points, and especially to discuss the infrared fixed-point behavior [7, 8]. We do not share the pessimistic attitude of Chýla et al. [7, 9] to the infrared results. If one believes in OPT, the infrared results, though quantitatively uncertain, are qualitatively unequivocal: We propose to take them at face value and compare them to experimental data [8].

The plan of this paper is as follows. Section II reviews OPT, and applies it to $R_{e^+e^-}$ in third order, with particular emphasis on the infrared limit. Section III compares the predicted $R_{e^+e^-}$ with experimental data, using Poggio-Quinn-Weinberg (PQW) smearing [10]. Section IV briefly discusses the phenomenology of a "frozen" couplant. Conclusions are summarized in Sec. V. Some technical matters are relegated to the appendices.

II. OPTIMIZED PERTUBATION THEORY AND FIXED-POINT BEHAVIOR

A. The principle of minimal sensitivity

We begin with a few words about the principle of minimal sensitivity, upon which OPT is based. It deals with any situation where an exact result is known to be independent of certain variables, but where the corresponding approximate result depends upon those variables, and hence is ambiguous. [In the QCD context, physical quantities are renormalization group (RG) invariant [11], but perturbative approximations to them are not, due to truncation of the perturbation series.] The philosophy is that such a noninvariant approximant is most believable where it is least sensitive to small variations in the extraneous variables, because this is where it best approximates the exact result's vital property of being completely insensitive to the extraneous variables.

A simple example is perhaps the best way to convey this idea. Consider the quantum-mechanical problem of computing the eigenvalues E_k of the quartic-oscillator Hamiltonian:

$$H = \tfrac{1}{2}p^2 + \lambda x^4,$$

(2.1)

where $[x, p] = i$. Suppose we do standard perturbation theory, but with [12]

$$H_0 = \tfrac{1}{2}(p^2 + \Omega^2 x^2), \quad H_{\rm int} = \lambda x^4 - \tfrac{1}{2}\Omega^2 x^2.$$

(2.2)

This introduces an "extraneous variable" Ω, and the approximate eigenvalues so calculated will be Ω dependent.

For example, first order for the kth eigenvalue gives

$$E_k^{(1)} = \frac{1}{2}(k + \tfrac{1}{2})\Omega + \frac{3\lambda}{4\Omega^2}(2k^2 + 2k + 1). \qquad (2.3)$$

However, we *know* that the exact eigenvalues are Ω independent. Therefore, it is sensible to choose Ω so that the approximant $E_k^{(1)}$ is minimally sensitive to Ω; i.e.,

$$\bar{\Omega} = \left[3\lambda \frac{2k^2 + 2k + 1}{k + \tfrac{1}{2}}\right]^{\frac{1}{3}}. \qquad (2.4)$$

(Quite generally, we shall use an overbar to denote an "optimized" value.) This gives the "optimized" result

$$E_k^{(1)}(\text{opt}) = \frac{3}{4}(k + \tfrac{1}{2})\left[3\lambda \frac{2k^2 + 2k + 1}{k + \tfrac{1}{2}}\right]^{\frac{1}{3}}. \qquad (2.5)$$

This simple formula fits the ground-state energy to 2% and *all* other energy levels to within 1%. The secret of this success is the "optimal" choice of Ω, which is different for different levels.

One may proceed to the calculation of higher-order corrections for some specific eigenvalue (e.g., the ground state, $k = 0$). For any fixed Ω the perturbation series would diverge, but if Ω is chosen in each order according to the "minimal sensitivity" criterion (which gives an $\bar{\Omega}$ that gradually increases with order), one finds quite nice convergence [12]. This is an example of the "induced-convergence" mechanism [5, 13].

One may also use the same method to obtain accurate approximate wave functions, $\psi_k(x)$, from first-order perturbation theory [14]. Here the "optimal" Ω will be a function of x; in particular, it will be proportional to $|x|$ at large $|x|$, thereby converting the Gaussian dependence $\exp(-\tfrac{1}{2}\Omega x^2)$ into the correct large-$|x|$ behavior. A variety of other examples and applications can be found in Refs. [3, 13, 15]. Some examples of QCD applications can be found in Refs. [16, 17].

B. RG invariance and optimization

We next review "optimized perturbation theory" (OPT) [3] as applied to the QCD corrections to the $R_{e^+e^-}$ ratio. Ignoring quark masses for the present, we may write $R_{e^+e^-} = 3\sum q_i^2(1 + \mathcal{R})$, where $\mathcal{R}$ has the form

$$\mathcal{R} = a(1 + r_1 a + r_2 a^2 + \cdots), \qquad (2.6)$$

and depends upon a single kinematic variable Q, the c.m. energy. OPT is based on the fundamental notion of RG invariance [11], which means that a physical quantity is independent of the renormalization scheme (RS). Symbolically, we can express this by

$$0 = \frac{d\mathcal{R}}{d(RS)} = \frac{\partial \mathcal{R}}{\partial(RS)} + \frac{da}{d(RS)}\frac{\partial \mathcal{R}}{\partial a}, \qquad (2.7)$$

where the total derivative is separated into two pieces corresponding to RS dependence from the series coefficients r_i and from the couplant, respectively. A particular case of Eq. (2.7) is the familiar equation expressing the renormalization-scale independence of $\mathcal{R}$:

$$\left(\mu\frac{\partial}{\partial\mu} + \beta(a)\frac{\partial}{\partial\mu}\right)\mathcal{R} = 0, \qquad (2.8)$$

where

$$\beta(a) \equiv \mu\frac{da}{d\mu} = -ba^2(1 + ca + c_2 a^2 + \cdots). \qquad (2.9)$$

The first two coefficients of the β function are RS invariant and, in QCD with N_f massless flavors, are given by

$$b = \frac{33 - 2N_f}{6}, \quad c = \frac{153 - 19N_f}{2(33 - 2N_f)}. \qquad (2.10)$$

When integrated, the β-function equation can be written as

$$\int_0^a \frac{da'}{\beta(a')} + \mathcal{C} = \int_{\tilde{\Lambda}}^\mu \frac{d\mu'}{\mu'} = \ln(\mu/\tilde{\Lambda}), \qquad (2.11)$$

where $\mathcal{C}$ is a suitably infinite constant and $\tilde{\Lambda}$ is a constant with dimensions of mass. The particular definition of $\tilde{\Lambda}$ that we use corresponds to choosing [3]

$$\mathcal{C} = \int_0^\infty \frac{da'}{ba'^2(1 + ca')} \qquad (2.12)$$

[where it is understood that the integrands on the left of (2.11) are to be combined before the bottom limit is taken]. This $\tilde{\Lambda}$ parameter is related to the traditional definition [18] by an RS-invariant, but N_f-dependent factor:

$$\ln(\Lambda/\tilde{\Lambda}) = (c/b)\ln(2c/b). \qquad (2.13)$$

The Λ parameter is scheme dependent, but the Λ's of different schemes can be related exactly by a one-loop calculation [19, 20]. As is usual, we shall regard $\Lambda_{\overline{\text{MS}}}$ (for four flavors) as the free parameter of QCD [21], where $\overline{\text{MS}}$ denotes the modified minimal subtraction scheme.

From Eq. (2.11) it is clear that a depends on RS only through the variables $\mu/\tilde{\Lambda}$ and $c_2, c_3, \ldots$, the scheme-dependent β-function coefficients. The coefficients of $\mathcal{R}$ can depend on RS only through these same variables, because of RG invariance, Eq. (2.7). Therefore, these variables provide a complete RS parametrization, as far as physical quantities are concerned [3]. Thus, we may write

$$a = a(\text{RS}) = a(\tau, c_2, c_3, \ldots), \qquad (2.14)$$

where

$$\tau \equiv b\ln(\mu/\tilde{\Lambda}). \qquad (2.15)$$

The τ variable is convenient and also serves to emphasize the very important point that RS dependence involves only the *ratio* of μ to $\tilde{\Lambda}$. "Optimization" does *not* determine an "optimum μ," but it will determine an optimum τ.

The dependence of a on the set of RS parameters τ and c_j [3] is most easily obtained [22] by taking partial derivatives of Eq. (2.11), varying one parameter while holding the others constant. This yields

$$\frac{\partial a}{\partial \tau} = \beta(a)/b, \qquad (2.16)$$

$$\frac{\partial a}{\partial c_j} \equiv \beta_j(a) = -b\beta(a) \int_0^a dx \, \frac{x^{j+2}}{[\beta(x)]^2}. \qquad (2.17)$$

Note that the β_j functions begin at order a^{j+1}.

The symbolic RG-invariance equation (2.7) can now be written out explicitly as the following set of equations:

$$\left(\frac{\partial}{\partial\tau}\bigg|_a + \frac{\beta(a)}{b} \frac{\partial}{\partial a} \right) \mathcal{R} = 0, \qquad (2.18)$$

$$\left(\frac{\partial}{\partial c_j}\bigg|_a + \beta_j(a) \frac{\partial}{\partial a} \right) \mathcal{R} = 0 \quad (j = 2, 3, \ldots). \qquad (2.19)$$

These equations determine how the coefficients r_i of $\mathcal{R}$ must depend on the RS variables. Thus, r_1 depends on τ only, while r_2 depends on τ and c_2 only, etc., with

$$\frac{\partial r_1}{\partial\tau} = 1, \qquad (2.20)$$

$$\frac{\partial r_2}{\partial\tau} = 2r_1 + c, \qquad \frac{\partial r_2}{\partial c_2} = -1, \qquad (2.21)$$

etc. Upon integration one will obtain $r_i = f(\tau, c_2, \ldots, c_i) + \text{const}$, where f is a known function and the constant of integration is a RS invariant. Thus, certain combinations of series coefficients and RS parameters,

$$\rho_1(Q) \equiv \tau - r_1, \qquad (2.22)$$

$$\rho_2 \equiv r_2 + c_2 - (r_1 + \tfrac{1}{2}c)^2, \qquad (2.23)$$

etc., are RS invariant [3, 23]. In the e^+e^- case, ρ_1 is a function of the c.m. energy Q, while ρ_2 and the higher-order invariants are pure numbers, dependent only on the number of flavors, N_f.

Although the exact $\mathcal{R}$ is RG invariant, the truncation of the perturbation series spoils this invariance. The nth-order approximant $\mathcal{R}^{(n)}$, defined by truncating $\mathcal{R}$ and the β function to only n terms, depends on the RS variables $\tau, \ldots, c_{n-1}$. OPT corresponds to choosing an "optimal" RS in which the approximant $\mathcal{R}^{(n)}$ is stationary with respect to RS variations, i.e., the RS in which $\mathcal{R}^{(n)}$ *exactly* satisfies the RG-invariance equations, (2.18) and (2.19). [Note that only the first $(n-1)$ equations will be nontrivial in nth order.]

The second-order approximant is

$$\mathcal{R}^{(2)} = a(1 + r_1 a), \qquad (2.24)$$

where a here is short for $a^{(2)}$, the solution to (2.11) with β truncated at second order. $\mathcal{R}^{(2)}$ depends on RS only through the variable τ. The optimization equation, from (2.18), is

$$\bar{a}^2 - \bar{a}^2(1 + c\bar{a})(1 + 2\bar{r}_1\bar{a}) = 0. \qquad (2.25)$$

This equation, together with the ρ_1 definition and the second-order integrated β-function equation, (2.11), uniquely determines the optimized result. (For details, see [3, 16].)

The third-order approximant is

$$\mathcal{R}^{(3)} = a(1 + r_1 a + r_2 a^2), \qquad (2.26)$$

where now a is short for $a^{(3)}$, the solution to (2.11) with β truncated at third order. $\mathcal{R}^{(3)}$ depends on RS through two parameters τ and c_2, so there are two optimization equations, coming from (2.18) and (2.19). These can be reduced to [3]

$$(3\bar{r}_2 + 2\bar{r}_1 c + \bar{c}_2) + (3\bar{r}_2 c + 2\bar{r}_1\bar{c}_2)\bar{a} + 3\bar{r}_2\bar{c}_2\bar{a}^2 = 0, \qquad (2.27)$$

$$I[1 + (c + 2\bar{r}_1)\bar{a}] - \bar{a} = 0, \qquad (2.28)$$

where

$$I = \int_0^{\bar{a}} \frac{dx}{(1 + cx + \bar{c}_2 x^2)^2}.$$

This integration can be done analytically, and is given by

$$I = \frac{1}{\Delta^2} \left[\frac{\bar{a}(c^2 - 2\bar{c}_2 + c\bar{c}_2\bar{a})}{(1 + c\bar{a} + \bar{c}_2\bar{a}^2)} - 4\bar{c}_2 f(\bar{a}, \bar{c}_2) \right], \qquad (2.29)$$

with

$$f(\bar{a}, \bar{c}_2) = \frac{1}{2\Delta} \ln \left[\frac{1 + \tfrac{1}{2}\bar{a}(c + \Delta)}{1 + \tfrac{1}{2}\bar{a}(c - \Delta)} \right], \qquad (2.30)$$

where $\Delta^2 \equiv c^2 - 4\bar{c}_2$. (This assumes that $\Delta^2 > 0$, which proves to be true here.) The procedure for solving these optimization equations is discussed further in Sec. II D, but next we discuss the infrared limit.

C. Infrared limit and fixed-point behavior

Suppose we consider $\mathcal{R}$ at lower and lower c.m. energy, Q. Since c is positive for $N_f \leq 8$, the second-order β function has no nontrivial zero. Thus, in any RS, the couplant $a^{(2)}$ and approximant $\mathcal{R}^{(2)}$ must become singular at some Q of order $\Lambda_{\overline{\text{MS}}}$. In third order this may or may not happen, depending on whether the RS has a positive or negative c_2. If c_2 is negative then the couplant remains finite and tends to a "fixed-point" value a^*, which is the nontrivial zero of the third-order β function, i.e., the positive root of

$$1 + ca^* + c_2 a^{*2} = 0. \qquad (2.31)$$

Since fixed-point behavior hinges on c_2, which is scheme dependent, it is vital to have a sensible choice of RS [6]. In OPT the optimal c_2 is determined by the optimization equations, and depends on Q somewhat. If $\bar{c}_2$ is negative as $Q \to 0$, then OPT will give a fixed-point behavior. The infrared limit of the optimization process was analyzed in Ref. [6] and we briefly review the relevant results.

Since β vanishes at a fixed point, the τ optimization equation, corresponding to (2.18), reduces to

$$1 + (2\bar{r}_1 + c)\bar{a}^* = 0. \qquad (2.32)$$

Then, just by differentiating (2.31) with respect to c_2, one obtains

$$\lim_{a \to a^*} \beta_2^{(3)}(a) = \frac{\partial a^*}{\partial c_2} = \frac{-a^{*2}}{c + 2c_2 a^*}. \qquad (2.33)$$

[This can also be obtained, more laboriously, as the limit of (2.17).] Thus, the c_2 optimization equation, corresponding to (2.19), becomes

$$\bar{a}^* + \frac{1 + 2\bar{r}_1\bar{a}^* + 3\bar{r}_2\bar{a}^{*2}}{c + 2\bar{c}_2\bar{a}^*} = 0. \tag{2.34}$$

The two optimization equations yield

$$\bar{r}_1 = -\frac{1}{2}\left(\frac{1 + c\bar{a}^*}{\bar{a}^*}\right), \quad \bar{r}_2 = -\frac{2}{3}\bar{c}_2. \tag{2.35}$$

Using the expression for the invariant ρ_2, (2.23), one obtains

$$\bar{c}_2 = 3\left(\rho_2 + \frac{1}{4\bar{a}^{*2}}\right). \tag{2.36}$$

Finally, substituting into the fixed-point condition (2.31), one finds [6]

$$\frac{7}{4} + c\bar{a}^* + 3\rho_2\bar{a}^{*2} = 0, \tag{2.37}$$

which determines $\bar{a}^*$ in terms of the RS-invariant quantities c and ρ_2. A positive $\bar{a}^*$ exists if ρ_2 is negative, and the more negative ρ_2 is, the smaller $\bar{a}^*$ will be.

D. Implementing the optimization procedure

Returning to finite Q, we now consider how to obtain the third-order optimized approximant $\bar{\mathcal{R}}^{(3)}$ numerically as a function of Q. As input, we need the values of ρ_1 and ρ_2. Being invariants, they can be obtained from calculations performed in any computationally convenient RS. The calculations in the literature have used the "modified minimal subtraction" ($\overline{\text{MS}}$) convention, with the renormalization point μ chosen to be Q. The $\mathcal{R}$ coefficients are [24, 2]

$$r_1(\overline{\text{MS}}; \ \mu = Q) = 1.9857 - 0.1153N_f, \tag{2.38}$$

$$r_2(\overline{\text{MS}}; \ \mu = Q) = -6.6368 - 1.2001N_f - 0.0052N_f^2$$
$$-1.2395\left(\sum q_i\right)^2 / \left(3\sum q_i^2\right). \tag{2.39}$$

The RS parameters of the $\overline{\text{MS}}(\mu = Q)$ scheme are

$$\tau(\overline{\text{MS}}; \ \mu = Q) = b\ln(Q/\tilde{\Lambda}_{\overline{\text{MS}}})$$
$$= b\ln(Q/\Lambda_{\overline{\text{MS}}}) + c\ln(2c/b), \tag{2.40}$$

$$c_2(\overline{\text{MS}}) = \frac{3}{16}\frac{1}{33 - 2N_f}\left[\frac{2857}{2} - \frac{5033}{18}N_f + \frac{325}{54}N_f^2\right]. \tag{2.41}$$

(The latter was first calculated in Ref. [25], and has recently been confirmed independently [26].) Substitution of these results into (2.22) and (2.23) gives the invariants. One can see explicitly that ρ_1 depends logarithmically on the c.m. energy Q, and on the free parameter of QCD, $\Lambda_{\overline{\text{MS}}}$ [21]. However, ρ_2 depends only on N_f. Since ρ_2 turns out to be negative, one will find fixed-point behavior in the "optimum" scheme [27, 28]. Table I gives the

TABLE I. ρ_2 invariants and fixed-point couplants for $N_f = 0$-6.

N_f	ρ_2	α_s^*/π
0	-8.410	0.313
1	-9.997	0.280
2	-10.911	0.263
3	-12.207	0.244
4	-13.910	0.224
5	-15.492	0.208
6	-17.665	0.191

fixed-point couplant values, determined from Eq. (2.37), for various N_f values [29].

Consider a world with N_f massless quarks, ignoring complications due to quark thresholds for the present. For simplicity we assume that the value of $\Lambda_{\overline{\text{MS}}}$ is given, and our numerical results use $\Lambda_{\overline{\text{MS}}} = 230$ MeV for four flavors [30]. For any chosen Q we then have definite numerical values for the invariant quantities ρ_1, ρ_2 (and b, c). We need to solve for the optimum couplant $\bar{a}$ and the optimized coefficients $\bar{r}_1$, $\bar{r}_2$, and this will involve determining the RS parameters $\bar{\tau}$, $\bar{c}_2$ of the optimal RS. These five variables are related by five equations: the two optimization equations, (2.27) and (2.28), the ρ_1, ρ_2 equations, (2.22) and (2.23), and the integrated β-function equation, (2.11), which for the β function truncated at third order becomes explicitly

$$\tau = \frac{1}{a} + c\ln(ca) - \frac{1}{2}c\ln(1 + ca + c_2a^2) - (c^2 - 2c_2)f(a, c_2),$$
$$\tag{2.42}$$

where $f(a, c_2)$ is given by (2.30). By substituting this last equation into the ρ_1 equation we can obtain $\bar{r}_1$ explicitly as a function of $\bar{a}$, $\bar{c}_2$. We can then rearrange the ρ_2 equation to give $\bar{r}_2$ explicitly as a function of $\bar{a}$, $\bar{c}_2$. This leaves $\bar{a}$, $\bar{c}_2$ to be solved for from the two optimization equations. Starting from an initial guess for a and c_2, our procedure was to solve (2.28) numerically for a new $\bar{a}$, and then (with the new $\bar{a}$) to solve (2.27) for a new $\bar{c}_2$. We then iterated this procedure until the difference between successive solutions reached a specified tolerance. Further details are given in Appendix A.

At very low Q we encountered technical problems with slow convergence of the iteration scheme. These are discussed in Appendix A. Nevertheless, with care it was possible to obtain accurate solutions at low energies. In Fig. 1 we show the optimized solution in the a,c_2 plane as it smoothly approaches the fixed-point solution, which lies on the infrared boundary $1 + ca + c_2a^2 = 0$. The figure shows two cases: $N_f = 3$ and $N_f = 2$. (In the real-world case we must switch from three flavors to two when we cross the strange-quark threshold. This requires a matching of Λ parameters, as discussed in Appendix B.)

The optimized couplant $\bar{a}$ is shown as a function of Q in Fig. 2. Note that the effective couplant below 300 MeV is nearly constant at about 0.263, which is the $N_f = 2$ fixed-point value. Figure 2 also shows the second- and third-order optimized results for $\mathcal{R}$. The second-order
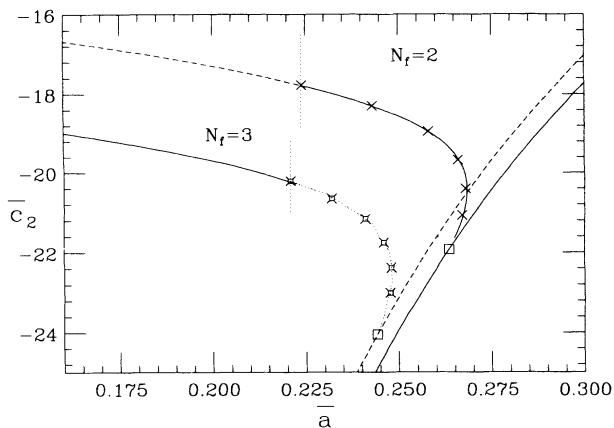
FIG. 1. The optimized solutions in the a, c_2 plane for two-
and three-quark flavors, in the low-energy region. The open
squares represent the fixed-point solution, Eqs. (2.37) and
(2.36), which lies on the infrared boundary $1 + ca + c_2 a^2 = 0$. The boundary is shown by the solid line ($N_f = 2$) or
the dashed line ($N_f = 3$) at the right. The dotted vertical
lines are to indicate $s\bar{s}$ threshold at $Q = 0.40$ GeV where
N_f changes from 3 to 2. [The Λ parameters are matched so
that $\bar{R}$ is continuous (see Appendix B), but there are then
slight discontinuities in $\bar{a}$ and $\bar{c}_2$.] The dotted line shows the
solution for a three-flavor world down to $Q = 0$, while the
dashed line shows a two-flavor world extending up towards 1
GeV. The points shown are spaced at 0.05 GeV intervals from
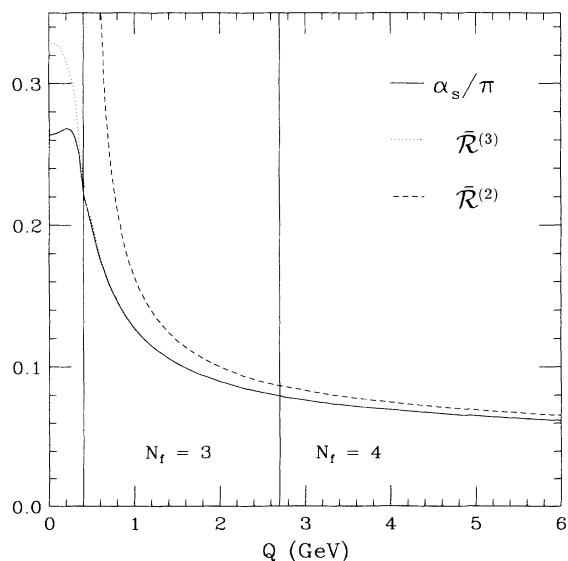$Q = 0.40$ GeV.

FIG. 2. The optimized third-order results for $\bar{a} = \alpha_s/\pi$
and $\bar{\mathcal{R}}^{(3)}$. Also shown is the second-order result, $\bar{\mathcal{R}}^{(2)}$. Quark
thresholds are indicated by the vertical lines.

result diverges at $Q \approx 400$ MeV, where $\rho_1(Q)$ vanishes.
However, $\bar{\mathcal{R}}^{(3)}$ remains finite, rising only to 0.33 at $Q = 0$.

E. Illustrative results

We pause for a moment to consider a comparison be-
tween the second- and third-order optimized results at
moderately high Q. This exercise was performed by sev-
eral authors [31, 32] when the "old" third-order result
[1] was first published, and the results were disquieting.
However, the new result [2] has transformed the situ-
ation, which is now very satisfactory. In Table II we
give details for the two illustrative cases considered by
Maxwell and Nicholls [31], namely $N_f = 5$, $Q = 34$ GeV,
with either $\tilde{\Lambda}_{\overline{\text{MS}}} = 100$ MeV or $\tilde{\Lambda}_{\overline{\text{MS}}} = 500$ MeV. (Note,
though, that the results depend only on the ratio of Q
to $\tilde{\Lambda}_{\overline{\text{MS}}}$.) From Table II we see that between second and
third order the optimized prediction $\mathcal{R}$ decreases only a
few percent. With the "old" result there had appeared
to be a disconcertingly large increase [31, 32]. The new
situation is much more satisfactory in other ways, too: In
both examples the coefficient $\bar{r}_2$ now has a more reason-
able magnitude, and the $\bar{r}_1$ coefficient has not changed
so drastically from second to third order.

The optimized couplant $\bar{a}$ now shows a marked de-
crease from second to third order. This is just what
one would expect in the "induced-convergence" picture
of Ref. [5]. In that picture "optimization" induces con-
vergence through a mechanism in which the effective ex-
pansion parameter $\bar{a}$ shrinks from one order to the next.
Note that the "old" result gave the opposite behavior,
with $\bar{a}$ apparently increasing from second to third order.

The results also shed some light on the error-estimation
question: If we knew just $\bar{\mathcal{R}}^{(2)} = \bar{a}(1+\bar{r}_1\bar{a})$, how might we
estimate the error? Two estimates suggest themselves:
(i) $n\bar{a}^3$, where n is an order-one number, which presumes
a well-behaved converging series, or (ii) $|\bar{r}_1\bar{a}^2|$, the mag-
nitude of the last calculated term, which is a typical error
estimate for an asymptotic series. Knowing $\bar{\mathcal{R}}^{(3)}$ we can,
presumably, get a much better idea of the actual error
in $\bar{\mathcal{R}}^{(2)}$ from the difference $\delta \equiv \bar{\mathcal{R}}^{(3)} - \bar{\mathcal{R}}^{(2)}$. We have
compared δ with estimates (i) and (ii) over a wide range
of $Q/\Lambda_{\overline{\text{MS}}}$ values.

Estimate (i), if we had assumed $n \approx 1$ or 2, would
have been rather too optimistic. In fact, $|\delta|$ is between 7
and 14 times $\bar{a}^3$ (for $N_f = 4$ and $Q/\Lambda_{\overline{\text{MS}}} \geq 5$). This is
directly related to the size of the invariant ρ_2 (which is
about -14 for four flavors). [One can show analytically
that $\delta = \rho_2\bar{a}^3 + O(\bar{a}^4)$ in the large-Q limit.] Of course,
we could not know ρ_2 until a third-order calculation was
done. Arguably, though, 14 can still be considered an
"order-one" number, especially in a theory that naturally
involves numbers such as four (flavors), three (colors),
eight (gluons), etc.

Estimate (ii), based on the last calculated term, agrees
with $|\delta|$ to within a factor of 2 either way for $Q/\Lambda_{\overline{\text{MS}}}$ be-
tween 5 and 1000. At higher $Q/\Lambda_{\overline{\text{MS}}}$ values this estimate
would be overly pessimistic. However, we think that for
present energies the estimate (ii) is perhaps the safest
way to estimate the error. We suggest that it be used

TABLE II.   Comparison of second- and third-order optimized results: "old" refers to third order with the old, incorrect result.

$N_f = 5$, $Q = 34$ GeV	Order	$\bar{a}$	$\bar{r}_1$	$\bar{r}_2$	$\bar{\mathcal{R}}$	Change
	Second	0.0415	−0.599	—	0.0404	—
$\tilde{\Lambda}_{\overline{MS}} = 100$ MeV	Third	0.0394	−0.301	7.64	0.0394	−2.4%
($\Lambda_{\overline{MS}} = 87$ MeV)	Old	0.0452	+1.363	−29.48	0.0453	12%
	Second	0.0569	−0.588	—	0.0550	—
$\tilde{\Lambda}_{\overline{MS}} = 500$ MeV	Third	0.0526	−0.405	7.71	0.0526	−4.4%
($\Lambda_{\overline{MS}} = 436$ MeV)	Old	0.0690	+1.988	−27.59	0.0694	26%

in QCD applications where only second-order results are known.

F. Credibility of the infrared results

We have stressed that OPT yields finite results for $\mathcal{R}$ down to $Q = 0$. The crucial question is, of course: How meaningful are these results? We would like to explain why, in contrast with other authors [7, 9, 33], we take a positive attitude on this issue.

First, suppose we adopt the philosophy that the last calculated term in the "optimized" perturbation series is a measure of the error. As we saw in this last section, this proved to be reasonable in the second-order case. In third order this gives $|\bar{r}_2 \bar{a}^3|$ as the error estimate. Since $\mathcal{R} \approx \bar{a}$, this implies a fractional error of $|\bar{r}_2 \bar{a}^2|$. In Table III we show some illustrative results at low energies, together with their estimated error. From this one can see that the behavior of the series is quite satisfactory above $Q = 1$ GeV. The situation undoubtedly deteriorates at lower energies; by the time we reach $Q = 0$ we have a series of the form $0.26(1 − 0.76 + 1.01)$ in which the higher-order terms are comparable to the leading term. While this is hardly a good situation, it is not completely disastrous; the corrections alternate in sign, and they do not dwarf the leading term. We believe that our error estimate, which grows to 100% at $Q = 0$, is not unreasonable: the result may well be off by a factor of 2, but is unlikely to be off by an order of magnitude. The qualitative conclusion that $\mathcal{R}$ remains small (say, 0.3 ± 0.3) at low energies is hard to escape.

Second, it is instructive to view the use of QCD perturbation theory in the infrared limit as an extrapolation

away from $N_f = 33/2$ [34]. At $N_f = 33/2$ the leading β-function coefficient b vanishes (and hence c goes to $−\infty$). For $N_f = 33/2 − \epsilon$, with ϵ small and positive, there must be an infrared fixed point at $a^* \sim −1/c = O(\epsilon)$ [34]. Perturbative calculations, even in the infrared, should then be meaningful if ϵ is sufficiently small. Furthermore, one could naturally expect that the more orders in perturbation theory one has, the further one can extrapolate from $N_f = 33/2$. With sufficient orders one should be able to get infrared results down to $N_f = 0$, unless there is some unknown reason for the behavior of the theory to change fundamentally at some critical N_f between $33/2$ and 0. What does happen? Well, at second order, of course, one finds fixed-point behavior, with $a^* = −1/c$, provided c is negative, which requires $N_f > 153/19 \approx 8$, though N_f needs to be still larger if a^* is to be reasonably small. In third order our results imply that, in the $R_{e^+e^-}$ case, fixed-point behavior, with moderately small a^* values, does extend to $N_f = 0$.

In the $\epsilon \rightarrow 0$ limit, a^* tends to $−1/c$, and hence to $(8/321)\epsilon$. The small coefficient suggests that the natural expansion parameter of an extrapolation from $N_f = 33/2$ is not ϵ but approximately $\epsilon/40$. One can verify that the third-order OPT results smoothly approach the limiting form as $\epsilon \rightarrow 0$. For $N_f = 16$ one has $\rho_2 = −1724.4$, and one gets a series of the form $0.012(1 − 0.03 + 0.04)$. As N_f decreases, the behavior of the series deteriorates, but it does so quite steadily; there is no dramatic change around $N_f = 8$ or any other N_f.

In conclusion, our view is that the $N_f = 2$ infrared results, while quantitatively uncertain, are qualitatively credible. Having made this case in theoretical terms, let us now see what experiment has to say.

TABLE III.   Illustrative third-order optimized results at low energies. $\Lambda_{\overline{MS}}$(4 flavors) $= 230$ MeV. The estimated fractional error is $|\bar{r}_2 \bar{a}^2|$.

Q (GeV)	N_f	$\bar{a}$	$\bar{r}_1$	$\bar{r}_2$	$\bar{\mathcal{R}}$	Error
3.0	4	0.076	−0.53	6.9	0.076	4%
1.0	3	0.126	−0.79	6.3	0.126	10%
0.4	3	0.221	−1.77	8.8	0.229	43%
0	2	0.263	−2.89	14.6	0.330	100%

III. COMPARING THEORY TO EXPERIMENT

A. $R_{e^+e^-}$ including quark masses

In this section we construct the theoretical prediction for $R_{e^+e^-}$ (allowing for quark masses) and discuss its comparison with experiment using the PQW smearing method. We limit ourselves to the region below 6 GeV, and we shall be particularly interested in the region below 1 GeV.

To allow for quark masses in $R_{e^+e^-}$, we used the approximate formula [10]

$$R_{e^+e^-} = 3 \sum_i q_i^2 \, T(v_i)[1 + g(v_i)\mathcal{R}], \qquad (3.1)$$

where the sum is over all quark flavors that are above threshold (i.e., whose masses, m_i, are less than $Q/2$), and

$$
\begin{aligned}
v_i &= (1 - 4m_i^2/Q^2)^{\frac{1}{2}}, \\
T(v) &= v(3 - v^2)/2, \\
g(v) &= \frac{4\pi}{3}\left[\frac{\pi}{2v} - \frac{3+v}{4}\left(\frac{\pi}{2} - \frac{3}{4\pi}\right)\right].
\end{aligned}
\qquad (3.2)
$$

The coefficient $T(v_i)$ is the parton-model mass dependence and $g(v_i)$ is a convenient approximate form for the mass dependence of the leading-order QCD correction [10, 35]. The higher-order corrections have been calculated only for massless quarks, so we simply evaluate $\mathcal{R}$ with N_f equal to the the number of above-threshold flavors.

In our numerical results we used standard values for the current-quark masses [36]: $m_u = 5.6$ MeV, $m_d = 9.9$ MeV, $m_s = 199$ MeV, $m_c = 1.35$ GeV. For $\Lambda_{\overline{\text{MS}}}$ we used a four-flavor value of 230 MeV above charm threshold ($Q > 2m_c$). Then, each time a flavor threshold was crossed as we decreased Q, we reduced N_f by 1 and computed the new $\Lambda_{\overline{\text{MS}}}$ parameter appropriate to the new N_f. The matching of Λ's is discussed in Appendix B.

In this way we obtained the "raw" theoretical prediction for $R_{e^+e^-}$ shown in Fig. 3. For comparison, the
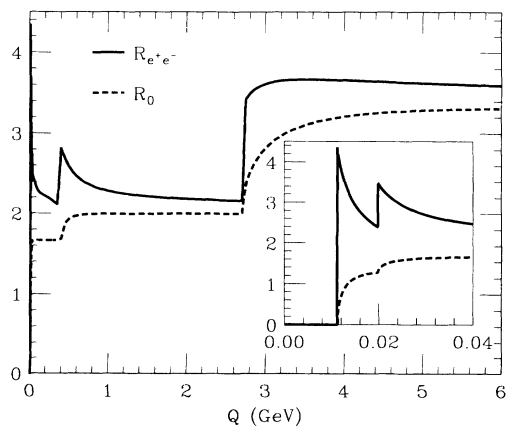

FIG. 3. The perturbative QCD prediction for $R_{e^+e^-}$ from third-order OPT (solid line). The inset shows the region around u and d quark thresholds. The dashed line is the parton-model prediction.

figure also shows the parton-model result (i.e., with the QCD correction term $\mathcal{R}$ set to zero).

B. PQW smearing

A *direct* comparison of the theoretical prediction with the experimental data is not possible, because there is no direct correspondence between the perturbative quark-antiquark thresholds and the hadronic thresholds and resonances of the data. However, a meaningful comparison is possible if some kind of "smearing" procedure is used [10, 37]. We used the smearing method of Poggio, Quinn, and Weinberg (PQW) [10], who define the "smeared" quantity

$$\bar{R}_{\text{PQW}}(Q; \Delta) = \frac{\Delta}{\pi} \int_0^\infty ds' \frac{R_{e^+e^-}(\sqrt{s'})}{(s' - Q^2)^2 + \Delta^2}. \qquad (3.3)$$

In terms of the vacuum-polarization amplitude Π, one can write $\bar{R}_{\text{PQW}}$ as [10]

$$2i\bar{R}_{\text{PQW}}(Q; \Delta) = \Pi(Q^2 + i\Delta) - \Pi(Q^2 - i\Delta). \qquad (3.4)$$

In the limit $\Delta \to 0$ this reduces to $2iR_{e^+e^-}$, which is the discontinuity of Π across its cut. However, a finite Δ keeps one away from the infrared singularities and nonperturbative effects that lurk close to the cut. The idea is to apply this smearing to both the theoretical and experimental $R_{e^+e^-}$'s and then compare them.

In principle, the more orders in perturbation theory one has, the smaller one can take Δ [10]. However, this requires the full mass dependence of the higher-order corrections, which we do not know. In their leading-order study of the charm-threshold region, PQW used a value $\Delta = 3$ GeV^2, and we shall use values of the same order of magnitude. We take a pragmatic view: the best choice of Δ is the smallest value that will smooth out any rapid variations in either the experimental or the theoretical $R_{e^+e^-}$. It turns out that this depends upon the energy region one is interested in. Around charm threshold a Δ of 3 GeV^2 or more is necessary, while in the lowest-energy region a Δ as small as 1 GeV^2 can be used.

The integral in Eq. (3.3) was evaluated by numerical integration, after first making a change of variables $s' - Q^2 = \Delta \tan \theta$. The computer routine was designed to take an input $R_{e^+e^-}$, specified over a range 0 to Q_{max} and to evaluate the integral over this range. A term was then added to account for the contribution from Q_{max} to ∞, assuming that $R_{e^+e^-}$ remained constant above Q_{max}. The accuracy of the numerical-integration routine was tested against analytic results for several simple input functions.

C. Experimental data and resonances

The experimental data we used come from a variety of sources: $e^+e^- \to \pi^+\pi^-$ data in the ρ region and above from the OLYA/CMD and DM2 Collaborations [38, 39]; Fraxati's ADONE collider $\gamma\gamma$2 data from 1.4 to 3 GeV [40]; SLAC Mark I data from 3 to 6 GeV [41]; and Crystal Ball data above 5 GeV [42]. For useful compilations and reviews see Ref. [43]. We used simple fits to the

data in some regions, particularly when the data had a lot of structure and/or had large statistical errors. This was more convenient for the numerical integration routine and made it easier for us to examine the effect of the experimental uncertainties on the smeared result. Figure 4 shows our data compilation, up to 6 GeV, excluding narrow resonances. In fact, we used data going well beyond b threshold, but they have no real effect on the results we present.

The sharp resonances ω, ϕ, J/ψ, ψ', and $\psi(3770)$ were not included in the data compilation so that their contribution to $\bar{R}_{\mathrm{PQW}}$ could be put in analytically. They have a relativistic Breit-Wigner form [44]

$$R_{\mathrm{res}} = \frac{9}{\alpha^2} B_{ll} B_h \frac{M^2 \Gamma^2}{(s - M^2)^2 + M^2 \Gamma^2}, \qquad (3.5)$$

where M, Γ, B_{ll}, and B_h are, respectively, the mass, width, leptonic branching fraction, and hadronic branching fraction of the resonance. The parameters for the resonances were taken from the 1992 Particle Data Group [36]. For B_{ll} we used the weighted average of the ee and $\mu\mu$ branching ratios.

The contribution of such a Breit-Wigner resonance to the smearing integral (3.3) can be evaluated analytically using partial fractions. [The resulting expression is too cumbersome to quote, but we may note that the narrow width approximation,

$$\frac{1}{(s - M^2)^2 + M^2 \Gamma^2} \approx \frac{\pi}{M\Gamma} \delta(s - M^2), \qquad (3.6)$$

which gives a contribution to $\bar{R}_{\mathrm{PQW}}$ of

$$\bar{R}_{\mathrm{res}} \approx \frac{9 B_{ll} B_h \Delta M \Gamma}{\alpha^2 [(s - M^2)^2 + \Delta^2]}, \qquad (3.7)$$

is a pretty good approximation.] In Fig. 5 we show, for two different Δ values, the contributions of the various resonances to the experimental $\bar{R}_{\mathrm{PQW}}$. The ρ's contribution is shown by a dotted line. However, since ρ is rather wide and asymmetric, it was actually treated, not in this manner, but by numerical integration, using the
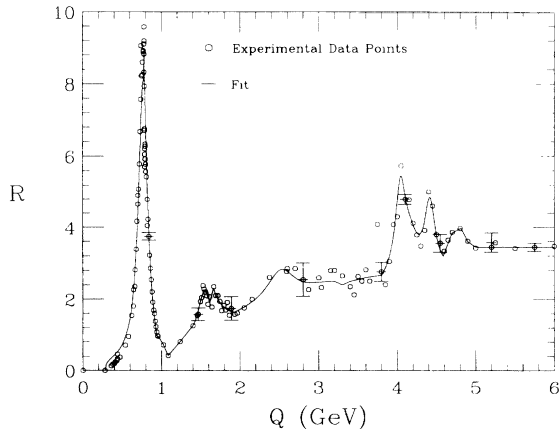

FIG. 4. Compilation of experimental $R_{e^+e^-}$ data (excluding narrow resonances). A few representative statistical error bars are shown. The solid line represents an "eyeball fit."
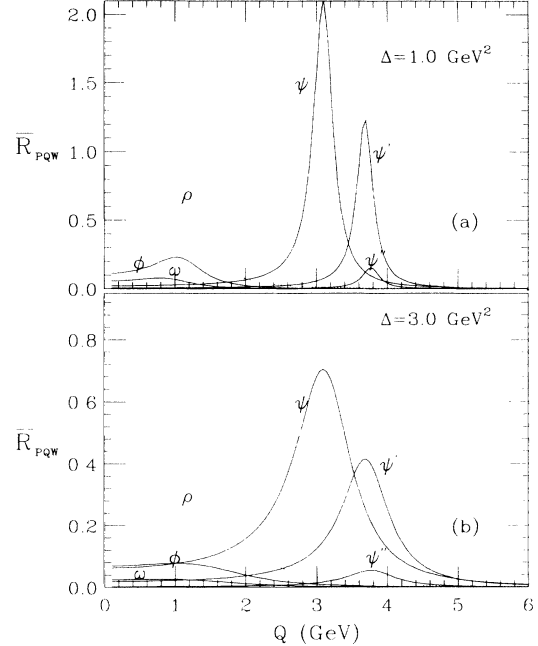

FIG. 5. The contributions of narrow resonances to $\bar{R}_{\mathrm{PQW}}$ for two values of the smearing parameter Δ.

data points from Ref. [38] as part of the data compilation (Fig. 4).

D. Results and uncertainty estimates

The results obtained by applying PQW smearing to both theory and experiment are shown in Fig. 6. For the smaller Δ (1 GeV^2) there is good agreement between theory and experiment below 1 GeV, but in the charm-threshold region there is clearly insufficient smearing for the comparison to be meaningful. Increasing Δ to 3 GeV^2 smooths out the experimental curve almost completely. The agreement between theory and experiment is excellent below 2 GeV. In the charm region the agreement is less good, but this can be attributed mainly to the sizable systematic normalization uncertainty (10–20 %) in the data in this region, which produces an uncertainty of about ± 0.4 in the experimental $\bar{R}_{\mathrm{PQW}}$ at around $Q = 4$ GeV. For comparison, Fig. 6(b) also includes the naive parton-model prediction. One can see from this that the QCD correction term $\mathcal{R}$ provides about a 20% increase which is vital to the good agreement with the data.

Using Q^2, rather than Q as the variable, we can continue $\bar{R}_{\mathrm{PQW}}(Q^2)$ into the negative Q^2 region (cf. Ref. [45]). As shown in Fig. 7, for $\Delta = 1$ GeV^2, the good agreement persists.

To quantify the good agreement at low energies, we discuss how various uncertainties would affect $\bar{R}_{\mathrm{PQW}}$ at $Q = 0$. First we discuss the experimental uncertainties. There is about a 5% uncertainty in the ρ, ω, and ϕ contributions, due to the uncertainty in their total and leptonic widths. For $\Delta = 1$ (3) GeV^2 this gives an error in $\bar{R}_{\mathrm{PQW}}(0)$ of about ± 0.04 (± 0.02). Uncertainties in the ψ resonance parameters affect $\bar{R}_{\mathrm{PQW}}(0)$ by ± 0.01 or less.
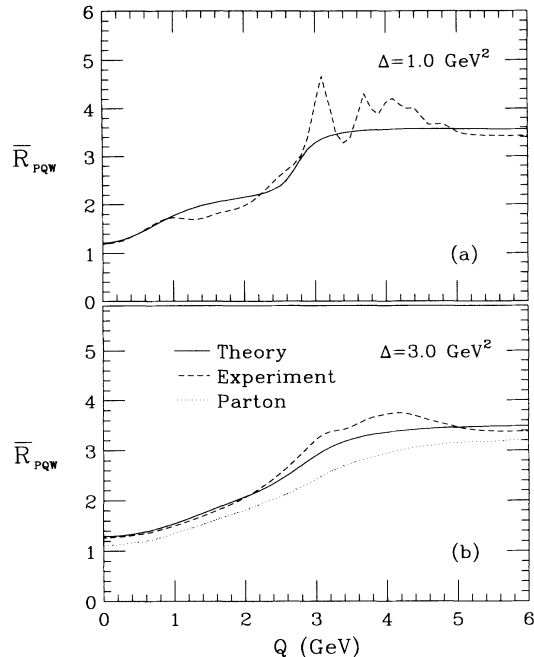
FIG. 6. Comparison of "smeared" theoretical and experimental results. The parton-model result is shown by the dotted line in (b).

We considered the effect of a 15% normalization change in the continuum data in the 1.5 – 3 GeV region: The effect on $\bar{R}_{PQW}(0)$ was about ±0.03 (±0.06) for $\Delta = 1$ (3) GeV^2. We also allowed for a 15% normalization change in the 3 – 5 GeV region. The effect on $\bar{R}_{PQW}(0)$ was about ±0.02 (±0.065) for $\Delta = 1$ (3) GeV^2. Combining these four distinct sources of error in quadrature, we estimate an overall uncertainty in the experimentally determined $\bar{R}_{PQW}(0)$ of ±0.06 for $\Delta = 1$ GeV^2 and ±0.08 for $\Delta = 3$ GeV^2.

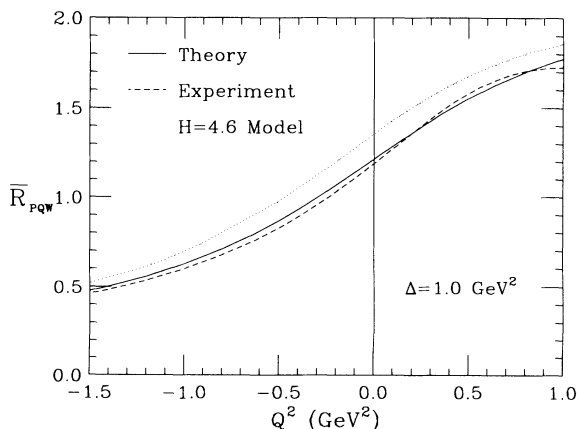On the theoretical side, errors arise from two sources: (i) uncertainty in the input parameters (quark masses

FIG. 7. Comparison of "smeared" results extended to spacelike Q^2. The dotted line shows a "straw-man" model in which the couplant becomes large at low energies (see Sec. III E).

and $\Lambda_{\overline{MS}}$), and (ii) truncation of the perturbation series. We varied each quark mass by its quoted error [36]. Varying the u and d masses had negligible effect. $\bar{R}_{PQW}(0)$ changed by ±0.004 (±0.001) on varying the s mass, and by ±0.005 (±0.013) on varying the c mass for $\Delta = 1$ (3) GeV^2. Changing $\Lambda_{\overline{MS}}$ by 50–280 MeV increased $\bar{R}_{PQW}(0)$ by 0.019 (0.014) for $\Delta = 1$ (3) GeV^2. The series-truncation error can reasonably be estimated from the last term in the optimized series, as we argued earlier. At 1 GeV this suggests that $\mathcal{R}$ is accurate to about 10%, and is considerably more accurate at larger energies. This is corroborated by the good agreement between second- and third-order results. The theoretical uncertainty in $\mathcal{R}$ above 1 GeV contributes an error in $\bar{R}_{PQW}(0)$ of less than ±0.006 (±0.009) for $\Delta = 1$ (3) GeV^2. Below 1 GeV the prediction for $\mathcal{R}$ is much more uncertain. However, as discussed in Sec. II F, we think that even at $Q = 0$ the result is reliable to within a factor of 2. Conservatively, we considered the effect of increasing the predicted $\mathcal{R}$ by a factor of 2 over the whole range, $0 < Q < 1$ GeV. This affects the low-energy $\bar{R}_{PQW}$ by 0.033 (0.011) for $\Delta = 1$ (3) GeV^2. If we linearly add all the above-mentioned uncertainties we get a total uncertainty of ±0.07 for $\Delta = 1$ GeV^2 and ±0.05 for $\Delta = 3$ GeV^2. Thus, the theoretical uncertainties are comparable to the experimental uncertainties.

E. Significance of the results

We can now discuss the significance of the agreement between theory and experiment. We first ask: How restrictive are the data? To quantify the discussion we define a "straw-man" model for $\mathcal{R}$ in which $\mathcal{R}$ is the same as the OPT result down to 2 GeV, but then follows the one-loop, three-flavor form, $(12/27)(1/\ln Q^2/\Lambda_0^2)$, with $\Lambda_0 \approx 0.2$ GeV, until it reaches a value H, at which it remains frozen down to $Q = 0$. If the "freezeout" value H is about 0.3, then this "H model" is essentially equivalent to the OPT result. If H is much larger then this model gives a result for $\bar{R}_{PQW}(0)$ that is too large by more than the uncertainties just estimated. We find that H's above 2 are disfavored by the data. (As an illustration Fig. 8 shows the result with $H = 4.6$, which is clearly ruled out.) At the other extreme, the data disfavor an H less than 0.09. Thus, although a wide range of H values can be tolerated, the data do imply that the couplant cannot grow very large in the infrared region, nor can it remain too small.

Next we ask: How predictive is the theory? Because of the need for smearing, the theory tells us almost nothing about the shape or structure of the e^+e^- data in the region below 1 GeV. However, it does tell us something about the average magnitude of the cross section. The low-energy data are, in fact, dominated by the ρ peak. After smearing with $\Delta = 1$ GeV^2, this contributes about 0.7 to $\bar{R}_{PQW}$ below 1 GeV. Thus a 10% change in the area under the ρ peak would change $\bar{R}_{PQW}$ by the ±0.07 estimated uncertainty in the theoretical prediction. We conclude that perturbative QCD can tell us, at least crudely, the size of the ρ resonance.
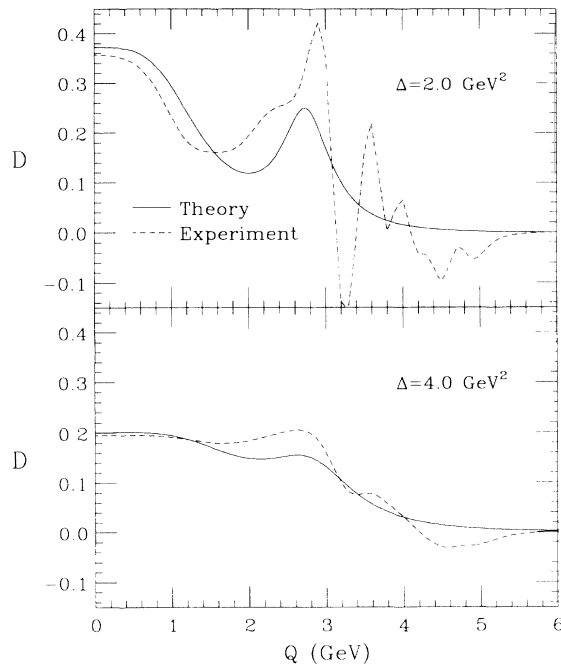
FIG. 8. Comparison of theoretical and experimental results for the "smeared derivative" [Eq. (3.8)] for two values of Δ.

F. The smeared derivative

As an extension of PQW's ideas we also considered a quantity

$$D(Q,\Delta) = \frac{2\Delta}{\pi} \int_0^\infty ds' \frac{R_{e^+e^-}(\sqrt{s'})(s'-Q^2)}{\{(s'-Q^2)^2 + \Delta^2\}^2}, \quad (3.8)$$

which represents a "smeared derivative," in the sense that

$$\lim_{\Delta \to 0} D(Q,\Delta) = dR_{e^+e^-}/dQ^2. \quad (3.9)$$

This provides a somewhat different test, though obviously not an independent test, of the relationship between theory and experiment. Its calculation requires only straightforward modifications to the procedures used to calculate $\bar{R}_{PQW}$.

In Fig. 8 we compare the smeared derivatives from theory and experiment for $\Delta = 2$ and 4 GeV^2. For $\Delta = 2$ GeV^2 there is good agreement at low energies, and the theory qualitatively gives the first peak just below 3 GeV. However, there is clearly insufficient smearing in the charm region. Increasing Δ to 4 GeV^2 greatly smooths out both curves and gives quite good agreement.

IV. PHENOMENOLOGICAL VIRTUES OF A FROZEN COUPLANT

The idea that the strong coupling constant $\alpha_s(Q^2)$ "freezes" at low energies has long been a popular and successful phenomenological hypothesis. We first note that a freezing of $\alpha_s(Q^2)$ is a natural consequence of a picture where the gluon aquires an effective, dynamical mass m_g [46]. Naively, this would modify the leading-

order, three-flavor couplant to

$$\frac{\alpha_s(Q^2)}{\pi} = \frac{12}{27} \frac{1}{\ln[(Q^2 + 4m_g^2)/\Lambda_0^2]}, \quad (4.1)$$

a form that has been used in many phenomenological papers. For m_g a little larger than Λ_0 this gives a zero-Q value comparable to ours. Note, though, that the variation with Q at low energies is somewhat different from ours in Fig. 2.

Another commonly used form is the "hard-freeze" form in which

$$\frac{\alpha_s(Q^2)}{\pi} = \begin{cases} (12/27)(1/\ln Q^2/\Lambda_0^2) & \text{for } Q^2 \geq Q_0^2, \\ \text{const} \equiv H & \text{for } Q^2 \leq Q_0^2, \end{cases} \quad (4.2)$$

with $H = (12/27)(1/\ln Q_0^2/\Lambda_0^2)$. This is the "$H$ model" that we mentioned in Sec. III E. For $H \approx 0.26$ (i.e., $Q_0/\Lambda_0 \approx 2.3$) it is a close approximation to our $\alpha_s(Q^2)/\pi$ shown in Fig. 2.

We now briefly survey some of the phenomenological literature in order to make two points: (i) a frozen α_s provides a way to understand many important facts in hadronic physics, and (ii) the values extracted phenomenologically are very much in accord with our low-Q value $\alpha_s/\pi = 0.26$. (Note that we quote α_s/π rather than α_s values.)

(a) *Total hadron-hadron cross sections*, although slowly rising at very high energies, are remarkably constant over a wide energy range, and their relative sizes correlate with their quark content in a very suggestive way. A simple and successful description is provided by the two-gluon-exchange model [47], based on the Low-Nussinov model of the Pomeron [48]. This model requires a finite couplant at low momentum transfer, and Ref. [47] found a value $\alpha_s/\pi \approx 0.17$. A recent version of this model, framed in terms of a dynamical gluon mass ($m_g = 0.37$ GeV, for $\Lambda_0 = 0.3$ GeV), is given in Ref. [49]. Another recent version of this model [50] uses the "H-model" form of $\alpha_s(Q^2)/\pi$. In order to fit the absolute magnitude of the π-nucleon cross section, Q_0 needs to be about 0.44 GeV [50] if $\Lambda_0 = 0.2$ GeV. This corresponds to $H = 0.28$. The same frozen couplant has been used successfully in subsequent work on deriving nucleon structure functions from the constituent-quark model [51].

(b) *Hadron spectroscopy* also points to a low-energy couplant of around 0.2 – 0.25 [52]. Godfrey and Isgur [53] provide a unified description of light- and heavy-meson properties in a "relativized" potential model with a universal one-gluon-exchange-plus-linear-confinement potential. For the model to work for light mesons it is crucial to incorporate relativistic effects, and to employ a form of the couplant that freezes at low energies. Their fits yield a form of $\alpha_s(Q^2)/\pi$ that freezes to about 0.19, and has a shape similar to ours. In a fully relativistic treatment Zhang and Koniuk [54] can naturally explain why π is so much lighter than ρ. The π/ρ mass ratio is a steeply falling function of the strong couplant, and the experimental value occurs at $\alpha_s/\pi = 0.265$ [54].

(c) *Hadron form factors* at low energies can be successfully treated assuming a frozen couplant, as shown in

Ref. [55], which used the form (4.1) with $m_g \approx 0.1$–0.5 GeV, for $\Lambda_0 \approx 0.1$ GeV.

(d) *Chiral soliton models of the nucleon* can fit a wide variety of nucleon properties if one includes one-gluon-exchange corrections with an α_s/π of about 0.2 [56, 57]. Reference [56] finds that the experimental deviation from the Gottfried sum rule, the Δ-nucleon mass difference, the first moment of the polarized proton structure function, and the neutron-proton mass difference all require a common α_s/π value. (However, the actual value found, 0.2, could be rescaled by making a different choice for another parameter in the model [56].) Other nucleon properties are consistent with an α_s/π of this size [57].

(e) *The p_T spectrum in W, Z production* in pp or $p\bar{p}$ collisions can be successfully predicted by QCD right down to $p_T = 0$ if multiple gluon radiation effects are appropriately resummed [58]. However, it is essential in the low-p_T region to invoke a freezing of $\alpha_s(p_T^2)$. The form (4.1) has been used, with $4m_g^2/\Lambda_0^2$ denoted by a. Unfortunately, the results are very insensitive to the parameter a; anything in the range $3 - 100$ gives an acceptable fit to current data [59, 60]. This corresponds to a range 0.1 $- 0.4$ for the zero-Q couplant. Perhaps future data will make it possible to narrow this range.

(f) *Jet properties* can be quite successfully described by the "modified leading log approximation" [61, 62], but to obtain predictions at small momenta it is necessary to invoke a freezing of the couplant. Fits to data on heavy-quark-initiated jets give zero-Q values of α_s/π around 0.22 [62]. This value depends somewhat on the form of $\alpha_s(Q^2)$ assumed in the fit, but it was found empirically that the result for the integral,

$$\int_0^{1 \text{ GeV}} dk \, \frac{\alpha_s^{\text{eff}}(k^2)}{\pi} \approx 0.2 \text{ GeV}, \qquad (4.3)$$

was *fit invariant* [62]. Integrating our α_s/π in Fig. 2 leads to precisely 0.2 GeV.

(g) *Hadron-hadron scattering at very high energies* where the cross sections rise asymptotically, but must satisfy unitarity, seems to call for the "critical Pomeron" picture [63], at least as a first approximation. It seems that one could only hope to derive such a picture from QCD if there is an infrared fixed point [64]. In fact, White has argued for additional quarks, or color-sextet quarks, in order to have N_f effectively equal to 16 [64]. (See the discussion in Sec. II F above.) However, our results imply that the infrared fixed point persists down to low N_f. This may mean that one can have all the virtues of White's picture without the need for more quarks.

V. SUMMARY AND CONCLUSIONS

We have applied OPT to the third-order QCD calculation of $R_{e^+e^-}$. At energies above about 1 GeV there is every sign that the approximation is healthy: the perturbation series in the "optimized" scheme is well behaved, and there is good agreement between second- and third-order results. This was not true of the situation created by the old, incorrect $R_{e^+e^-}$ calculation [1, 31, 32] (see Table II). The contrast between the "old" and "new" results

emphasizes the point that the third-order $R_{e^+e^-}$ calculation provides a very real, empirical test of "optimization" ideas. At the time, the statements [32] that the "old" third-order results [1] tended to cast doubt on the usefulness of "optimization" were perfectly fair comments. Because of this history we take special satisfaction in the transformed situation produced by the new result [2].

Furthermore, contrary to the old situation, the optimized couplant now shows a marked decrease from second to third order. This is in accord with the "induced-convergence" conjecture that "optimization" naturally cures the divergent-series problem [5, 13].

The third-order OPT results remain finite down to $Q = 0$, with the optimized couplant, α_s/π, "freezing" to a value 0.26 below 300 MeV. No *ad hoc* assumption was used to obtain this result: it is the direct consequence of using the calculated $R_{e^+e^-}$ and β series coefficients as inputs to the "optimization" procedure specified in Ref. [3].

It must be admitted that, at very low energies, the prediction for $\mathcal{R}$ (the QCD correction term in $R_{e^+e^-}$) has a large uncertainty. Since third order is the lowest order at which it is even possible to get finite infrared results, one should not be surprised if the approximation is somewhat crude. Nevertheless, as we discussed in Sec. II F, the qualitative conclusion that $\mathcal{R}$ remains small (say, 0.3 ± 0.3 at $Q = 0$) is inescapable in the context of OPT.

The OPT prediction is supported by the data. As we showed in Sec. III, the PQW-smeared $R_{e^+e^-}$ data are consistent with a perturbative QCD description, provided that the couplant freezes to a modest value at low energies.

The hypothesis that the couplant freezes at low energies has been used very successfully in a wide variety of phenomenological work, where the low-energy couplant is treated as a free parameter to be fitted to experiment. The values that emerge are quite comparable to ours. There are some other theoretical indications of a freezing of the couplant [46, 65], but our evidence is remarkable in that it comes solely from perturbation theory and RG invariance. The predicted value, $\alpha_s/\pi = 0.26$, for the frozen couplant is a purely theoretical number. It does not depend on knowing the value of $\Lambda_{\overline{\text{MS}}}$, but only on knowing the number of light quarks.

APPENDIX A: NUMERICAL SOLUTION OF THE OPTIMIZATION EQUATIONS

After expressing $\bar{r}_1$ and $\bar{r}_2$ in terms of $\bar{a}$ and $\bar{c}_2$, using the ρ_1, ρ_2 definitions and (2.42), we have to simultaneously solve the optimization equations, (2.27) and

(2.28). These define two curves in the a,c_2 plane whose intersection point we seek. In what we call the "spiralling" method, (2.28) is first solved for $\bar{a}$; then, with this $\bar{a}$, (2.27) is solved for $\bar{c}_2$; then, with this $\bar{c}_2$, (2.28) is solved for $\bar{a}$; and so on. Which equation is solved for which variable is crucial; the other choice would "spiral out" from the desired solution. (The standard "secant method" [66] was generally sufficient for solving the individual optimization equations.)

A convenient starting point for this iterative procedure was provided by an approximate solution to the optimized equations due to Pennington, Wrigley, Mignaco, and Roditi (PWMR) [67]. This approximation expands the optimization equations (2.27) and (2.28) as a series in $\bar{a}$ and keeps only the lowest nontrivial term. Noting that $I = \bar{a}(1 - c\bar{a} + \cdots)$, it is easy to check that this gives

$$\bar{r}_1 \approx 0, \quad \bar{r}_2 \approx -\tfrac{1}{3}\bar{c}_2. \tag{A1}$$

One can improve this approximation by writing each $\bar{r}_i$ as a series in $\bar{a}$ and successively equating coefficients of different orders in $\bar{a}$ to zero. To next order this gives

$$\bar{r}_1 \approx \tfrac{1}{3}\bar{c}_2\bar{a}, \quad \bar{r}_2 \approx -\tfrac{1}{3}\bar{c}_2 + \tfrac{1}{9}c\bar{c}_2\bar{a}. \tag{A2}$$

(One may note that in $\bar{\mathcal{R}}^{(3)}$ there is a near cancellation between the second- and third-order terms, $\bar{r}_1\bar{a}$ and $\bar{r}_2\bar{a}^2$. Thus, $\bar{\mathcal{R}}^{(3)}$ turns out to be closely equal to $\bar{a}^{(3)}$.)

The "spiralling" method worked well for $Q > 0.3$ GeV starting from the PWMR solution. However, at lower energies the PWMR approximation breaks down, and does not provide a satisfactory initial guess. In fact, at the infrared fixed point one has instead, from (2.35),

$$\bar{r}_1 = \tfrac{1}{2}\bar{c}_2\bar{a}^*, \quad \bar{r}_2 = -\tfrac{2}{3}\bar{c}_2. \tag{A3}$$

We therefore proceeded to low Q in successive stages, utilizing the solution at the previous Q as the initial guess for the next lower Q. We also encountered a "creep" problem: At low Q the two curves representing the "optimization" equations become almost parallel (each being almost parallel to the infrared boundary line $1 + ca + c_2a^2 = 0$) and they cross at a very small angle. Thus, instead of "spiralling in" to the solution, one creeps towards it stepwise. The convergence is very slow and the danger is that the solution can appear to have converged within the specified tolerance, when in fact it still has a considerable way to go. To avoid this pitfall we would repeat the procedure from a different starting point, so as to creep towards the solution from the other side. In this way we could bracket the true solution, and hence ensure reliable accuracy.

We also tried the "intersection" method as an alternative. Taking an initial guess for $\bar{c}_2$, one solves for $\bar{a}$ in each of the two optimized equations. For each $\bar{a}$ one then solves the other equation for $\bar{c}_2$. This gives a pair of points on each of the two curves. The straight lines that join up each pair should approximate the curves themselves, and hence their intersection should approximate the desired solution. The procedure can then be iterated. This method also worked well for $Q > 0.3$ GeV starting from the PWMR solution. At lower energies, where the two curves become nearly parallel, this method did not suffer from the "creep" problem, but it had the opposite vice: it tended to make such a large extrapolation in each iteration that it would become unstable and erratic.

APPENDIX B: FLAVOR THRESHOLDS

Since $\mathcal{R}$ has been calculated only with massless quarks, we are really approximating "full QCD" with a *set* of effective theories, each with a different number of massless quarks. The $\Lambda_{\overline{\text{MS}}}$ parameters of these theories need to be appropriately matched, so that they correspond to a single, underlying "full QCD" theory. The point is well explained by Marciano [68], who provides explicit formulas for matching $\Lambda_{\overline{\text{MS}}}$ across thresholds. Unfortunately his analysis uses a truncated expansion of $a(\mu)$ in powers of $1/\ln(\mu/\Lambda)$, which would not be a valid approximation at low energies, in particular at s-quark threshold.

Our procedure was simply to require the optimized $\bar{\mathcal{R}}^{(3)}$ to be continuous at a threshold. This was done numerically by running our optimization program at the threshold energy ($Q = 2m_q$) with both values of N_f and adjusting one of the $\Lambda_{\overline{\text{MS}}}$ parameters until the two $\bar{\mathcal{R}}^{(3)}$ results agreed. Starting with $\Lambda_{\overline{\text{MS}}}^{(4)} = 230$ MeV for 4 flavors, we found $\Lambda_{\overline{\text{MS}}}^{(3)} = 281$ MeV, and $\Lambda_{\overline{\text{MS}}}^{(2)} = 255$ MeV. (In terms of $\tilde{\Lambda}$ the corresponding values are 257, 308, and 277 MeV for 4, 3, and 2 flavors, respectively.) Essentially the same results were obtained if we required instead that $\bar{a}$ be continuous. We checked that this procedure agreed very closely with Marciano's formulas at both c- and b-quark thresholds.

It is noteworthy that we find $\Lambda_{\overline{\text{MS}}}^{(2)}$ to be smaller than $\Lambda_{\overline{\text{MS}}}^{(3)}$, contrary to the pattern at the higher thresholds. Our final results are very insensitive to the $\Lambda_{\overline{\text{MS}}}^{(2)}$ value, however, because at energies below s threshold the $\mathcal{R}$ results are essentially governed by the infrared fixed point.

[1] S. G. Gorishny, A. L. Kataev, and S. A. Larin, Phys. Lett. B **212**, 238 (1988).

[2] L. R. Surguladze and M. A. Samuel, Phys. Rev. Lett. **66**, 560 (1991); S. G. Gorishny, A. L. Kataev, and S. A. Larin, Phys. Lett. B **259**, 144 (1991).

[3] P. M. Stevenson, Phys. Rev. D **23**, 2916 (1981).

[4] These questions were originally posed by P. M. Stevenson (private communication to Dr. Gorishny, Dr. Kataev, and Dr. Larin, 1988), before the original $R_{e^+e^-}$ calculation was completed.

[5] P. M. Stevenson, Nucl. Phys. **B231**, 65 (1984).

[6] J. Kubo, S. Sakakibara, and P. M. Stevenson, Phys. Rev. D **29**, 1682 (1984).

[7] J. Chýla, A. Kataev, and S. Larin, Phys. Lett. B **267**,

269 (1991).

[8] Our main results have been briefly presented in A. C. Mattingly and P. M. Stevenson, Phys. Rev. Lett. **69**, 1320 (1992); in *The Fermilab Meeting*, Proceedings of the Annual Meeting of the Division of Particles and Fields of the APS, Batavia, Illinois, 1992, edited by C. Albright, H. Kasper, R. Raja, and J. Yoh (World Scientific, Singapore, 1993).

[9] See also, in the context of fixed-point behavior in the QCD calculation of the hadronic Higgs decay width, S. G. Gorishny, A. L. Kataev, S. A. Larin, and L. R. Surguladze, Phys. Rev. D **43**, 1633 (1991).

[10] E. C. Poggio, H. R. Quinn, and S. Weinberg, Phys. Rev. D **13**, 1958 (1976).

[11] E. C. G. Stueckelberg and A. Peterman, Helv. Phys. Acta **26**, 449 (1953); M. Gell-Mann and F. Low, Phys. Rev. **95**, 1300 (1954).

[12] W. Caswell, Ann. Phys. (N.Y.) **123**, 153 (1979); J. Killingbeck, J. Phys. A **14**, 1005 (1981); E. J. Austin and J. Killingbeck, *ibid.* **15**, L443 (1982).

[13] An "induced-convergence" mechanism has been proved to operate in the linear δ expansion: I. R. C. Buckley, A. Duncan, and H. F. Jones, Phys. Rev. D **47**, 2554 (1993); A. Duncan and H. F. Jones, *ibid.* **47**, 2560 (1993).

[14] S. K. Kauffmann and S. M. Perez, J. Phys. A **17**, 2027 (1984).

[15] H. F. Jones and M. Monoyios, Int. J. Mod. Phys. A **4**, 1735 (1989); J. O. Akeyo and H. F. Jones, *ibid.* **4**, 1668 (1989); J-H. Pei, C. M. Dai, and D. S. Chuu, Surf. Sci. **222**, 1 (1989); P. M. Stevenson, Phys. Rev. D **24**, 1622 (1981).

[16] D. W. Duke and J. D. Kimel, Phys. Rev. D **25**, 2960 (1982); D. W. Duke and R. G. Roberts, Phys. Rep. **120**, 275 (1985).

[17] P. Aurenche, R. Baier, and M. Fontannaz, Z. Phys. C **48**, 143 (1990); P. Aurenche, R. Baier, M. Fontannaz, J. F. Owens, and M. Werlen, Phys. Rev. D **39**, 3275 (1989).

[18] W. A. Bardeen, A. J. Buras, D. W. Duke, and T. Muta, Phys. Rev. D **18**, 3998 (1978).

[19] W. Celmaster and R. J. Gonsalves, Phys. Rev. D **20**, 1420 (1979).

[20] Two schemes, which for the same μ value are related by $a' = a(1+v_1 a+\cdots)$, have Λ parameters which are related by $\ln(\Lambda'/\Lambda) = v_1/b$. This relation is *exact* [19,3].

[21] The choice of $\Lambda_{\overline{MS}}$ as the free parameter of QCD is an arbitrary choice, but a harmless one since the Λ of any other "reference scheme" could be related *exactly* to $\Lambda_{\overline{MS}}$ (see [20] above). Thus, this choice affects only how the predictions are parametrized, and not their content. For complications related to flavor thresholds, see Appendix B.

[22] H. D. Politzer, Nucl. Phys. **B194**, 493 (1982).

[23] Some authors use a different definition: $\bar{\rho}_2 = \rho_2 + \frac{1}{4}c^2$.

[24] K. G. Chetyrkin, A. L. Kataev, and F. V. Tkachov, Phys. Lett. **85B**, 277 (1979); M. Dine and J. Sapirstein, Phys. Rev. Lett. **43**, 668 (1979); W. Celmaster and R. J. Gonsalves, Phys. Rev. D **21**, 3112 (1980).

[25] O. V. Tarasov, A. A. Vladimirov, and A. Yu. Zharkov, Phys. Lett. **93B**, 429 (1980).

[26] S. A. Larin and J. A. M. Vermaseren, Phys. Lett. B **303**, 334 (1993).

[27] Fixed-point behavior will also be found in RS's which are sufficiently close to the "optimized" scheme. This is the case, for instance, in the "fastest apparent convergence"

(FAC) or "effective charge" scheme (the RS in which $r_1 = r_2 = 0$). However, this scheme gives an a^* that is 64% larger than ours, for $N_f = 2$.

[28] The π^2 term in r_2 [2] gives a substantial negative contribution to ρ_2. Another timelike process, hadronic decay of the Higgs boson, also has a sizable, negative ρ_2: see Ref. [9] and references therein. In a spacelike case, deep-inelastic scattering, the third-order QCD corrections to the Gross–Llewellyn Smith, and Bjorken sum rules give ρ_2's that are negative only for $N_f \geq 4$ or 5. [See S. A. Larin and J. A. M. Vermaseren, Phys. Lett. B **259**, 345 (1991).] It may be that in this case fixed-point behavior will extend to fewer flavors only in higher orders. Alternatively, it might be that there is a real difference in behavior between spacelike and timelike processes. Another possibility is that exponentiation of some of the π^2 contributions is important. [See, e.g., G. Parisi, Phys. Lett. **90B**, 295 (1980); A. P. Contogouris, S. Papadopoulos, and J. P. Ralston, Phys. Rev. D **25**, 1280 (1982).] The adaptation of OPT to partially exponentiated approximants is discussed in Sec. VI D of Ref. [3].

[29] It is noteworthy that the fixed-point values all lie comfortably below the classical critical value $\frac{9}{8\pi} = 0.358$ of J. Mandula, Phys. Lett. **67B**, 175 (1977).

[30] Obviously, the procedure may be repeated with different trial values of $\Lambda_{\overline{MS}}$ if one seeks to determine the value that gives the best fit to the $R_{e^+e^-}$ data.

[31] C. J. Maxwell and J. A. Nicholls, Phys. Lett. B **213**, 217 (1988).

[32] A. P. Contogouris and N. Mebarki, Phys. Rev. D **39**, 1464 (1989); G. Altarelli, in *The Rice Meeting*, Proceedings of the Annual Meeting of the Division of Particles and Fields of the APS, Houston, Texas, 1990, edited by B. E. Bonner and H. E. Miettinen (World Scientific, Singapore, 1990).

[33] J. Chýla, Phys. Rev. D **38**, 3845 (1988).

[34] T. Banks and A. Zaks, Nucl. Phys. **B196**, 189 (1982); A. Zee, Phys. Rev. Lett. **48**, 295 (1982).

[35] J. Schwinger, *Particles, Sources, and Fields* (Addison-Wesley, New York, 1973), Vol. II, Chap. 5-4.

[36] Particle Data Group, K. Hikasa *et al.*, Phys. Rev. D **45**, S1 (1992).

[37] R. M. Barnett, M. Dine, and L. McLerran, Phys. Rev. D **22**, 594 (1980).

[38] OLYA/CMD Collaboration, L. M. Barkov *et al.*, Nucl. Phys. **B256**, 365 (1985).

[39] DM2 Collaboration, D. Bisello *et al.*, Phys. Lett. B **220**, 321 (1989).

[40] $\gamma\gamma2$ Collaboration, C. Bacci *et al.*, Phys. Lett. **86B**, 234 (1979).

[41] Mark I Collaboration, J. L. Siegrist *et al.*, Phys. Rev. D **26**, 969 (1982).

[42] Crystal Ball Collaboration, C. Edwards *et al.*, SLAC Report No. SLAC-PUB-5160, 1990 (unpublished).

[43] Particle Data Group, J. J. Hernández *et al.*, Phys. Lett. B **239**, 1 (1990), p. III.7A; J. P. Perez-y-Jorba and F. M. Renard, Phys. Rep. C **31** (1977); G. J. Feldman and M. L. Perl, *ibid.* **33** (1977); R. F. Schwitters and K. Strauch, Annu. Rev. Nucl. Sci. **26**, 89 (1976).

[44] See, e.g., V. Barger and R. J. N. Phillips, *Collider Physics* (Addison-Wesley, New York, 1987), Chap. 4.

[45] S. L. Adler, Phys. Rev. D **10**, 3714 (1974).

[46] J. M. Cornwall, Phys. Rev. D **26**, 1453 (1982); G. Parisi and R. Petronzio, Phys. Lett. **94B**, 51 (1980).

[47] J. F. Gunion and D. E. Soper, Phys. Rev. D **15**, 2617 (1977).

[48] F. Low, Phys. Rev. D **12**, 163 (1975); S. Nussinov, Phys. Rev. Lett. **34**, 1268 (1975).

[49] F. Halzen, G. I. Krein, and A. A. Natale, Phys. Rev. D **47**, 295 (1992).

[50] N. N. Nikolaev and B. G. Zakharov, Z. Phys. C **49**, 607 (1991); **53**, 331 (1992).

[51] V. Barone, M. Genovese, N. N. Nikolaev, E. Predazzi, and B. G. Zakharov, Int. J. Mod. Phys. A **8**, 2779 (1993); Z. Phys. C **58**, 541 (1993).

[52] T. Barnes, Z. Phys. C **11**, 135 (1981); T. Barnes, F. E. Close, and S. Monaghan, Nucl. Phys. **B198**, 380 (1982), Sec. 5.

[53] S. Godfrey and N. Isgur, Phys. Rev. D **32**, 189 (1985).

[54] T. Zhang and R. Koniuk, Phys. Lett. B **261**, 311 (1991).

[55] C.-R. Ji and F. Amiri, Phys. Rev. D **42**, 3764 (1990).

[56] J. Stern and G. Clement, Nucl. Phys. **A504**, 621 (1989); Phys. Lett. B **264**, 426 (1991).

[57] I. Duck, Phys. Rev. C **47**, 1751 (1993); L. R. Dodd and D. E. Driscoll, *ibid.* **47**, 1791 (1993).

[58] G. Altarelli, R. K. Ellis, M. Greco, and G. Martinelli, Nucl. Phys. **B246**, 12 (1984).

[59] R. S. Fletcher, F. Halzen, A. Grau, G. Pancheri, and Y. N. Srivastava, Phys. Lett. B **237**, 113 (1990).

[60] We thank Dr. R. S. Fletcher for helpful correspondence on this issue.

[61] Yu. L. Dokshitzer, V. A. Khoze, and S. I. Troyan, Lund Report No. LU TP 92-10 (unpublished).

[62] V. Khoze, in *Proceedings of the XXVIth International Conference on High Energy Physics*, Dallas, Texas, 1992, edited by J. Sanford, AIP Conf. Proc. No. 272 (AIP, New York, 1993).

[63] A. A. Migdal, A. M. Polyakov, and K. A. Ter Martirosyan, Zh. Eksp. Teor. Fiz. **67**, 84 (1974) [Sov. Phys. JETP **40**, 43 (1975)]; H. D. I. Abarbanel and J. B. Bronzan, Phys. Rev. D **9**, 2397 (1974).

[64] A. R. White, Phys. Rev. D **29**, 1435 (1984); in *Hadronic Matter in Collision*, edited by J. Rafelski (World Scientific, Singapore, 1989).

[65] V. N. Gribov, Lund Report No. LU-TP 91-7, 1991 (unpublished).

[66] W. H. Press, B. P. Flannery, S. A. Teukolsky, and W. T. Vetterling, *Numerical Recipes (Fortran Version)* (Cambridge University Press, Cambridge, England, 1989).

[67] M. R. Pennington, Phys. Rev. D **26**, 2048 (1982); J. C. Wrigley, *ibid.* **27**, 1965 (1983); see also P. M. Stevenson, *ibid.* **27**, 1968 (1983); J. A. Mignaco and I. Roditi, Phys. Lett. **126B**, 481 (1983).

[68] W. J. Marciano, Phys. Rev. D **29**, 580 (1984).